GEOPHYSICS, VOL. 59, NO. 10 (OCTOBER 1994); P. 1500–1511, 9 FIGS., 2 TABLES.

Multichannel Wiener deconvolution of vertical seismic profiles

Jakob B.U. Haldorsen*, Douglas E. Miller‡, and John J. Walsh**

ABSTRACT

We describe a technique for performing optimal, least-squares deconvolution of vertical seismic profile (VSP) data. The method is a two-step process that involves (1) estimating the source signature and (2) applying a least-squares optimum deconvolution operator that minimizes the noise not coherent with the source signature estimate. The optimum inverse problem, formulated in the frequency domain, gives as a solution an operator that can be interpreted as a simple inverse to the estimated aligned signature multiplied by semblance across the array. An application to a zero-offset VSP acquired with a dynamite source shows the effectiveness of the operator in attaining the two conflicting goals of adaptively spiking the effective source signature and minimizing the noise.

Signature design for seismic surveys could benefit from observing that the optimum deconvolution operator gives a flat signal spectrum if and only if the seismic source has the same amplitude spectrum as the noise.

INTRODUCTION

VSP data are normally collected with a seismic source at the surface and one or more geophones in the borehole. The data recorded by a downhole receiver can be viewed as a superposition of a downgoing field generated by the source at the surface and altered by transmission effects in the medium, an upcoming field, and noise not related to the source. The upgoing wavetrain can be regarded as the response of the earth beneath the receivers to a perturbation caused by the complicated downgoing field, making the downgoing field the "effective" seismic source. A deconvolution operator that collapses the effective signature will recover the impulse response of the lower-lying earth from the upgoing wavetrain.

From vertical seismic profile (VSP) data, one can get a good estimate of the effective source field close to a reflector. Everything aligned with the direct arrival can be treated reasonably as part of the source signature. Previous research (e.g., Kennet et al., 1980; DiSiena et al., 1980; Seeman and Horowitz, 1983 ; Hardage, 1985), has concentrated on the downgoing estimation problem, treating the deconvolution design as a separate, single-channel problem to be solved by standard techniques. Conventionally, the multichannel estimation of a downgoing wave is followed by the application of a deconvolution filter, designed at each level as the inverse of the estimated downgoing signal.

In this paper, we adopt an alternative viewpoint, treating the estimation of the deconvolution filter itself as the object of the multichannel design problem. Our formal approach is close to that of Berkhout (1977), who described multichannel deconvolution design for application to surface seismic data. The downgoing source field is estimated from a vertical array of receivers, similar to the methods of Kennet et al. (1980) and Hardage (1985). As we estimate the source field, we also find an optimum inverse filter. This filter is an intrinsically stable Wiener deconvolution filter where the spectral energy of the noise is determined implicitly. Our method is a direct extension of a processing algorithm developed for the deconvolution of seismic data acquired with a drill-bit source The drill-bit method is described by Miller et al. (1990) and Haldorsen et al. (1992).

The noise-optimal deconvolution filter can be written as a conventional inverse to the average downgoing signal weighted at each frequency by the semblance across the receiver array at that frequency. These two terms help the filter attain the two conflicting objectives of adaptive11 spiking the direct arrivals and of minimizing the noise incoherent with these arrivals. We will compare this formula lation to "conventional" deconvolution processing where the noise attenuation is achieved by adding white noise and

Manuscript received by the Editor April 14, 1993; revised manuscript received April 11, 1994.
*Geco Prakla, Buchholzerstrasse 100, D-30655 Hannover 51, Germany.
‡Schlumberger-Doll Research, Old Quarry Road, Ridgefield, CT.
**Schlumberger Cambridge Research, High Cross, Madingley Road, Cambridge, CB3-OEL, England.

by applying a subsequent band-limiting filter. In an application to a zero-offset VSP recorded with a dynamite source, we will see how the noise attenuation is achieved automatically by the optimum deconvolution filter without the subjective and labor-intensive filter testing that is required by conventional deconvolution.

DATA MODEL

We assume that each trace s,(t) contains noise $\mathcal{N}_n(t)$ added to a signal f(t). The signal is delayed by the transit time t_n between the source and the receivers. Under these assumptions we write

$$s_n(t) = f(t - t_n) + \mathcal{N}_n(t). \tag{1}$$

For VSP data acquired with an impulsive source, t_n is determined by picking first arrivals. For a vibrator source, the initial values of t_n will be found from the correlated data, using the synthetic sweep as an initial estimate of the source signature.

In equation (1), f is the "effective" source signature; i.e., the signature of the surface source complicated by the transmission through the earth. The noise term represents both uncorrelated random noise and reflected signal that is coherent with the source but with a different moveout across the array.

The processing algorithm will be based on equation (1) in its frequency-domain version:

$$s_n(\omega) = f(\omega)e^{i\omega t_n} + \mathcal{N}_n(\omega). \tag{2}$$

SIGNATURE ESTIMATION

We want the estimate of the signal that corresponds to maximum signal energy-or minimum noise energy. The average noise energy is given by

$$E_{\mathcal{N}}(\omega) = \frac{1}{N}\sum_{n=1}^{N} |\mathcal{N}_n(\omega)|^2, \tag{3}$$

where N is the number of traces (offsets, levels) contained within the window in which the signature is stable.

Solving equation (2) for $\mathcal{N}_n(\omega)$ and substituting, we get, after some elementary manipulation:

$$E_{\mathcal{N}}(\omega) = \frac{1}{N}\sum_{n=1}^{N} |s_n(\omega)e^{-i\omega t_n} - f(\omega)|^2, \tag{4}$$

and the value of f(o) that minimizes the noise energy is

$$\hat{f}(\omega) = \frac{1}{N}\sum_{n=1}^{N} s_n(\omega)e^{-i\omega t_n}. \tag{5}$$

The signature estimate $\hat{f}(\omega)$ is the average trace along a moveout path described by t_n. This is, in principle, the same method that Kennet et al. (1980) and Hardage (1985) describe for estimating the downgoing source field. For noisy data one may consider replacing the average expressed in equation (5) by the median of the moveout-aligned traces (Hardage, 1985).

We find the bias of the signature estimate from equations (5) and (2):

$$\hat{f}(\omega) - f(\omega) = \frac{1}{N}\sum_{n=1}^{N} \mathcal{N}_n(\omega)e^{-i\omega t_n}. \tag{6}$$

Provided that the right-hand side of equation (6) is zero; i.e.,

$$\frac{1}{N}\sum_{n=1}^{N} \mathcal{N}_n(\omega)e^{-i\omega t_n} = 0, \tag{7}$$

$\hat{f}$ is an unbiased estimate off. The condition (7) characterizes the noise.

DECONVOLUTION FILTER

Having found an estimate of the source signature corresponding to a minimum noise energy in the raw data [equation (5)], we want to find a deconvolution filter that collapses the source signature to a spike. At the same time, we want this filter to leave the least noise energy in the deconvolved data. In this section we will find a Wiener deconvolution filter that is completely determined by the data and the model in equation (2).

Optimum inverse filter

After the application of the deconvolution filter F(w), the average noise energy $E_{F\mathcal{N}}(\omega)$ is

$$E_{F\mathcal{N}}(\omega) = \frac{1}{N}\sum_{n=1}^{N} |F(\omega)\mathcal{N}_n(\omega)|^2$$

$$= E_{\mathcal{N}}(\omega)|F(\omega)|^2, \tag{8}$$

where $E_{\mathcal{N}}(\omega)$ is given by equation (3).

We can define the error energy associated with the failure of the deconvolution filter to "spike," or spectrally whiten the signal spectrum by

$$E_{err}(\omega) = |1 - F(\omega)f(\omega)|^2. \tag{9}$$

Using $\hat{f}$ from equation (5) as the signal means that any energy that satisfies condition (7) will be considered noise. With data that have been correctly sampled spatially, given the moveout difference between the downgoing and upcoming energy, the reflected energy will thus be considered "noise," and $E_{F\mathcal{N}}$ and E_{err} will not be independent. A filter that attempts to minimize both $E_{F\mathcal{N}}$ and E_{err} will preserve the part of $\mathcal{N}_n$ that is spectrally coherent with f. Our optimum filter F(w) is therefore found by minimizing

$$\Lambda(\omega; F) = E_{F\mathcal{N}}(\omega) + E_{err}(\omega)$$

$$= E_{\mathcal{N}}(\omega)|F(\omega)|^2 + |1 - F(\omega)\hat{f}(\omega)|^2. \tag{10}$$

Here we have replaced $f(\omega)$ by $\hat{f}(\omega)$, assuming that equation (7) holds.

The derivative of A with respect to F is

$$\frac{\partial\Lambda(\omega; F)}{\partial F} = 2F^*(\omega)E_{\mathcal{N}}(\omega) - 2[1 - F^*(\omega)\hat{f}^*(\omega)]\hat{f}(\omega), \tag{11}$$

and the value of F(o) that minimizes the sum of the noise and error energies becomes

$$F(\omega) = \frac{\hat{f}^*(\omega)}{|\hat{f}(\omega)|^2 + E_{\mathcal{N}}(\omega)}, \quad (12)$$

where we use * for "complex conjugate." This filter will reduce the noncoherent noise and compress and enhance any energy that is spectrally coherent with $\hat{f}$.

Wiener deconvolution filters, similar to expression (12), can be derived in a number of different ways [e.g., for seismic processing, Berkhout (1977); for restoration of blurred images, Andrews and Hunt (1977, 126-140)].

Equation (12) cannot be used directly as it requires an estimate of the energy spectrum of the noise. Interchanging f(o) and $\hat{f}(\omega)$ [with the condition (7)], it is easily seen from equations (4) and (5) that

$$E_{\mathcal{N}}(\omega) = \frac{1}{N}\sum_{n=1}^{N} |s_n(\omega)|^2 - |\hat{f}(\omega)|^2, \quad (13)$$

which introduced into equation (12) simplifies this to

$$F(\omega) = \frac{\hat{f}^*(\omega)}{E_T(\omega)}, \quad (14)$$

where $E_T(\omega)$ is the average total energy of the raw traces:

$$E_T(\omega) = \frac{1}{N}\sum_{n=1}^{N} |s_n(\omega)|^2. \quad (15)$$

In equation (14), the implicit determination of the noise-spectrum from the trace model (2) has replaced the explicit determination suggested by equation (12).

We can rearrange the terms in equation (14) to give

$$F(\omega) = \frac{\hat{f}^*(\omega)}{|\hat{f}(\omega)|^2} S(\omega), \quad (16)$$

where the frequency-domain semblance S(w) is given by

$$S(\omega) = \frac{|\hat{f}(\omega)|^2}{E_T(\omega)}. \quad (17)$$

We recognize the first factor $\hat{f}^*(\omega)/|\hat{f}(\omega)|^2$ in equation (16) as a spiking deconvolution filter. The spiking deconvolution filter is modified by the semblance S(w) . The semblance acts as a data adaptive band-limiting filter attenuating frequencies where the signal-to-noise ratio is small.

One could imagine implementing the filter (16) as a cascaded filter: a conventional deconvolution followed by semblance weighting. This may give almost identical results, provided the signal spectrum has no zeros, in which case the cascaded filter becomes indeterminate. If the filter is implemented in its simplest form, according to equation (14), any zeros in f(o) will not constitute a problem.

In analogy with a suggestion by Hardage (1985) for the estimation of the source signature from noisy data, one may consider replacing the average total energy in equation (14) by the median total energy.

Stability of the optimum inverse

The average total energy of the deconvolved traces can be determined using equations (16), (17), and (15):

$$E_{FT}(\omega) = \frac{1}{N}\sum_{n=1}^{N} |F(\omega)s_n(\omega)|^2$$
$$= |F(\omega)|^2 E_T(\omega)$$
$$= S(0). \quad (18)$$

The stability of F(w) is ensured by equation (18) as $0 \le S(0) \le 1$.

DECONVOLUTION OF THE SIGNAL

The filter designed using equations (5) and (14) will transform a signal of any shape and phase characteristics into a zero-phase, band-limited wavelet.

From equation (16), we find that $F(\omega)$ applied to the estimate $\hat{f}(\omega)$ of the signal gives the signal-amplitude:

$$g(\omega) = F(\omega)\hat{f}(\omega)$$
$$= S(0). \quad (19)$$

The least-squares best estimates of the source signature and its inverse are given by $\hat{f}(\omega)$ and F(w). With S(w) ≠ 1, equation (19) demonstrates that the best estimate of the inverse off(o) is not the inverse of the best estimate off(o). (Note: $S(\omega) = 1$ when $\mathcal{N}(\omega) = 0$.)

In the time domain, g(t) is a zero-phase, symmetric time series with a peak at $t = 0$, since the spectrum is composed of real-valued numbers S(w). We get the peak amplitude from equation (19) by Fourier transformation:

$$g(t = 0) = S_0, \quad (20)$$

where S_0 is the average frequency-domain semblance:

$$S_0 = \frac{1}{N_\omega}\sum_{\omega} S(\omega). \quad (21)$$

N_ω is the number of frequency samples.

Source signature optimization

It follows from equation (19) that the least-squares opti mum deconvolution algorithm gives a deconvolved signature with a flat spectrum if and only if the seismic source has the same amplitude spectrum as the noise. dur best source is thus not necessarily the source with the flattest spectrum but the source that has the same spectrum as the noise. This observation has obvious applications in signature design, ir particular with vibrators where the signature can be designed to fit the particular noise environment.

EFFECTIVE BANDWIDTH OF THE SIGNAL

If the semblance S(w) is constant and equal to α over a frequency interval $\Delta\Omega$ and zero outside this interval, the average semblance S_0 calculated over a larger frequency interval Ω, becomes

$$S_0 = \frac{\alpha \Delta\Omega}{\Omega}. \quad (22)$$

The frequency-averaged total energy after deconvolution is $\alpha\Delta\Omega/\Omega$ [follows from equation (18)] and the average signal energy is $\alpha^2 \Delta\Omega/\Omega$ [follows from equation (19)]. This gives a ratio of signal energy to total energy of α. Given that the measured ratio between the signal energy and total energy is $\alpha_{s/T}$, we can define an "effective" bandwidth $\Delta\Omega_e$ of the signal in analogy with equation (22). Substituting $\alpha_{s/T}$ for α and $\Delta\Omega_e$ for $\Delta\Omega$ and rearranging terms, we get

$$\Delta\Omega_e = \frac{S_0}{\alpha_{S/T}} \Omega. \quad (23)$$

$\Delta\Omega_e$ has the intuitively correct properties that $\Delta\Omega_e = \Omega$ when $S_0 = 1$ ($\Rightarrow \alpha = 1$) and $\Delta\Omega_e \rightarrow 0$ as $S_0 \rightarrow 0$. $S_0 = 1$ means that there is no noise in the data, and $S_0 = 0$ that there is no signal.

MEASURES OF NOISE AND SIGNAL

We summarize the estimators for the energy of signal and noise in the data, before and after application of F(w) in Table 1. N_ω is the number of frequency samples. After deconvolution, the total energy is given by equation (18). To find the signal energy expressed in terms of $S(\omega)$ and $E_T(\omega)$, we used equations (17) and (19). The noise energy is found by subtracting the signal energy from the total energy.

Calculating the energies listed in Table 1 helps in evaluating the data as well as the performance of the algorithm. One measure of the performance of the filter *on the average* is the increase in the signal-to-total-energy ratio. However, for data giving a nonflat semblance spectrum, the visual effect may be significant even for small changes in this ratio.

One can note that while the semblance $S(\omega)$ remains unchanged by the deconvolution, the total energy is changed to S(w), a number between 0 and 1. We also have the condition that the average semblance is less than the signal-to-total-energy ratio because some bands - of frequencies included in the processing may contain little or no energy. These frequencies will reduce the value of the average semblance but will have little effect on the signal-to-total-energy ratio calculated according to Table 1. If the spectrum of the semblance is flat; i.e., the noise and the signal have the same spectra, the average semblance will be equal to the signal-to-total-energy ratio.

For random and uncorrelated noise, the energy will be evenly distributed over the entire record after deconvolution filtering; whereas, the signal will be compressed. This will give an amplitude ratio of signal to noise that is significantly higher than what can be calculated from the expression in Table 1.

APPLICATION: A ZERO OFFSET VSP

We will look at an application to a zero-offset VSP to study the effect of the semblance weighting. For this purpose, we will show two separate processings of the data where the only difference is the introduction of semblance weights. The data are good quality, and we found indistinguishable results whether we used average or median estimators for the signatures and energy spectra.

Data

The data were recorded with a Schlumberger SAT* Seismic Array Tool, using dynamite sources placed approximately 100 m from the wellhead. The raw stack of the VSP is shown in Figure 1. The amplitude spectra of the full-length data traces (Figure 2) show that most of the energy is concentrated in a frequency range of 5 to 35 Hz with a rapid decay in amplitude above 35 Hz. Although weak, there is still energy at higher frequencies, and one of the objectives of the deconvolution is to bring out the signal at these frequencies.

*Mark of Schlumberger.

Table 1. Absolute and relative energies of signal and noise, before and after deconvolution.

	Before Deconvolution	After Deconvolution
Total energy	$E_T(\omega)$	$S(\omega)$
Signal energy	$S(\omega)E_T(\omega)$	$S(\omega)S(\omega)$
Noise energy	$(1 - S(\omega))E_T(\omega)$	$(1 - S(\omega))S(\omega)$
Average semblance	$\frac{1}{N_\omega}\sum_\omega S(\omega)$	$\frac{1}{N_\omega}\sum_\omega S(\omega)$
Signal-to-total energy	$\frac{\sum_\omega S(\omega)E_T(\omega)}{\sum_\omega E_T(\omega)}$	$\frac{\sum_\omega S(\omega)S(\omega)}{\sum_\omega S(\omega)}$
Signal-to-noise energy	$\frac{\sum_\omega S(\omega)E_T(\omega)}{\sum_\omega (1 - S(\omega))E_T(\omega)}$	$\frac{\sum_\omega S(\omega)S(\omega)}{\sum_\omega (1 - S(\omega))S(\omega)}$

The break times t_n were found by picking the first breaks on the raw data traces. The source signature was estimated in a moving window of five receivers. The application of the algorithm assumes that the source signature does not change over the trace window considered, which imposes a constraint upon the maximum length of the receiver array. The estimated signature was assigned to the central trace within the window. Figure 3 shows, in an arbitrary time reference, the signatures obtained using equation (5). Corrected for traveltimes, the signatures give an estimate of the direct field (Figure 4).

The frequency-domain semblance S(w) is found as the ratio of the energy in the estimated direct wave to the total energy averaged across the array of receivers within the moving trace window. The semblance is shown in Figure 5. The low values of the semblance around 50 Hz suggest a strong presence of noise at this frequency, probably generated by the rig and associated equipment on the surface. We arbitrarily chose to process frequencies from 0 to 105 Hz.

Figure 6a shows the spectra of the traces after deconvolution using a simple, conventional spiking deconvolution filter. Figure 6b shows the corresponding spectra following the application of the optimal inverse filter. The conventional filter is implemented by setting $S(\omega) = 1$ in equation (16) and adding enough white noise (0.01 percent) to the denominator to stabilize the filter.

Examination of the spectra in Figure 6 shows that the introduction of the semblance weights into the inverse filter has given an operator that is less sensitive to noise in the data. The semblance weights provide a data-adaptive band-limiting filter. In particular, the 50-Hz noise seen in the raw data has been attenuated by the semblance weights.

The deconvolution filters were applied directly to the unseparated data. The result is shown in Figure 7. The subtraction of the deconvolved source field leaves the deconvolved reflected field shown in Figure 8. This is the postfiltering residual of the "noise" N in the data model (2). The optimum inverse filter has attenuated (or failed to magnify) the incoherent noise, leaving the mostly coherent, reflected energy. The signal reflected from deeper flat layers was aligned in a conventional way by shifting the traces by twice the break times. The aligned reflected signal was enhanced using a moving-average filter over five receivers. This procedure is analogous to the way we estimated the downgoing source field. The enhanced, look-ahead VSP images are shown in Figure 9.

The only difference between the processing leading to the two sets of look-ahead VSP images in Figure 9 is the application of the frequency-domain semblance. The noise-limiting property of the optimum inverse filter becomes evident when comparing the two VSP images. Both VSP sections have a significantly higher resolution than the surface seismic. The surface seismic data are 48-fold, recorded using 25-m spacing of the receiver groups and 50-m source spacing. A geophone group consisted of a pattern of 24 vertical geophones. The seismic source was a stack of eight 8-s, 16-80-Hz sweeps by three vibrators. The data have been migrated using the generalized radon transform (GRT) algorithm described in Miller et al. (1987).

Bandwidth, relative signal, and noise energy

We have used the expressions listed in Table 1 when calculating the relative signal and noise energies in Table 2. Table 2 gives the frequency-averaged semblance, signal-to-total and signal-to-noise-energy ratios before and after the

(text continues on page 1510)

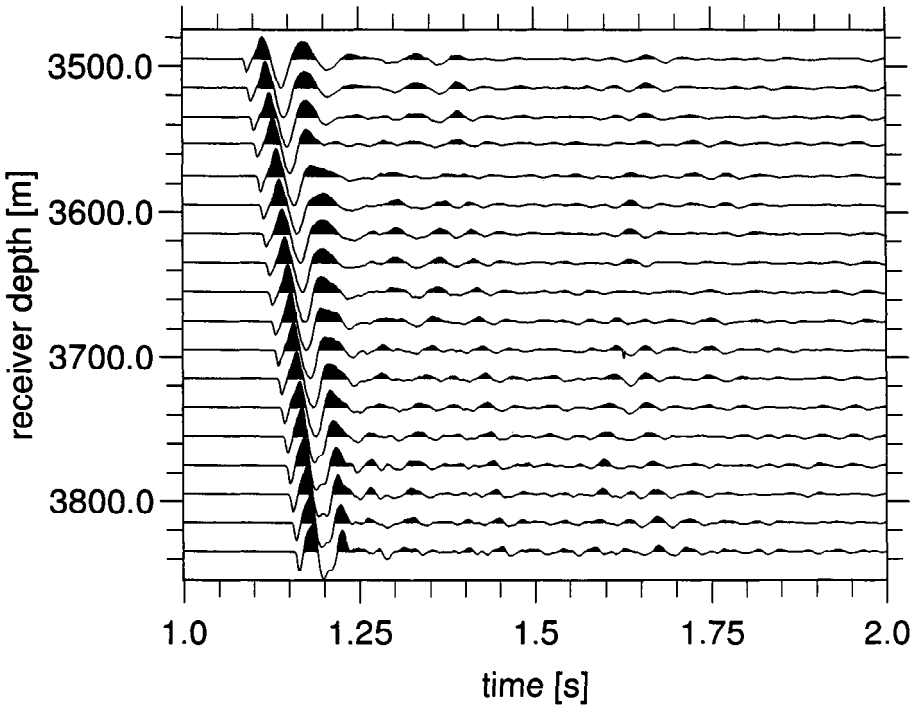

FIG. 1. Stacked raw vertical component VSP data. Each trace in the display is individually normalized.

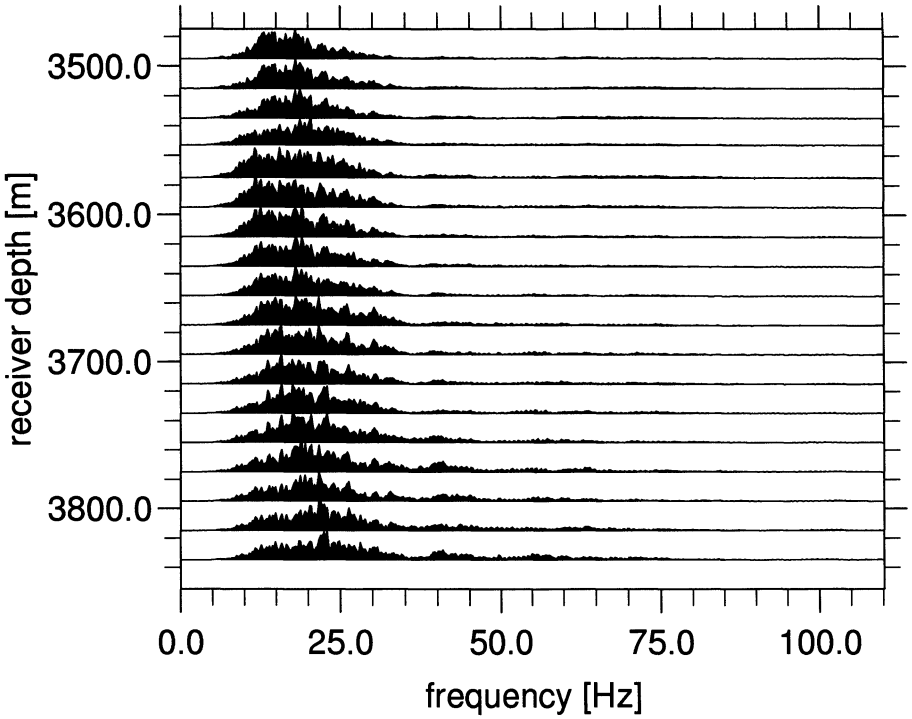

FIG. 2. Amplitude spectra of raw data from Figure 1. Each spectrum is individually normalized.

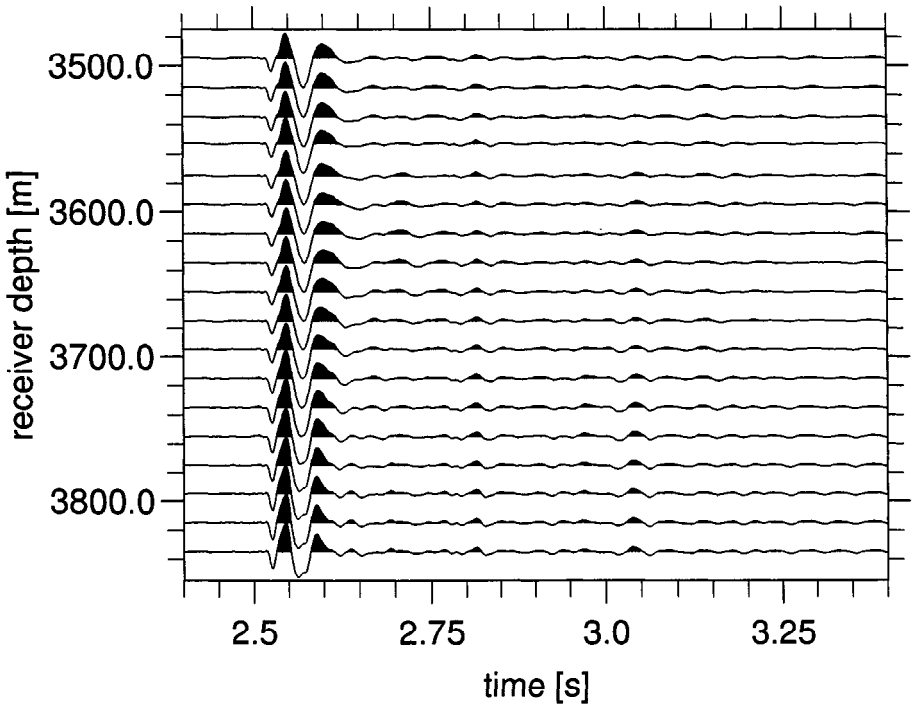

FIG. 3. Estimated signatures obtained using equation (5) in a five-trace sliding window. Traces are individually normalized.

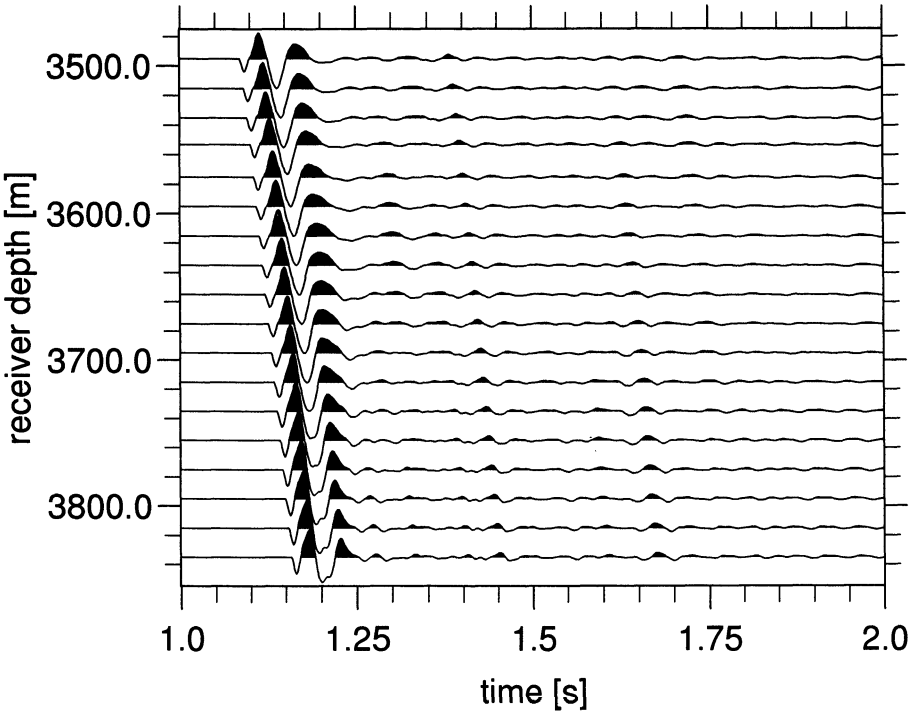

FIG. 4. The estimated direct field showing the signatures from Figure 3 corrected for traveltime. Display is normalized trace by trace.

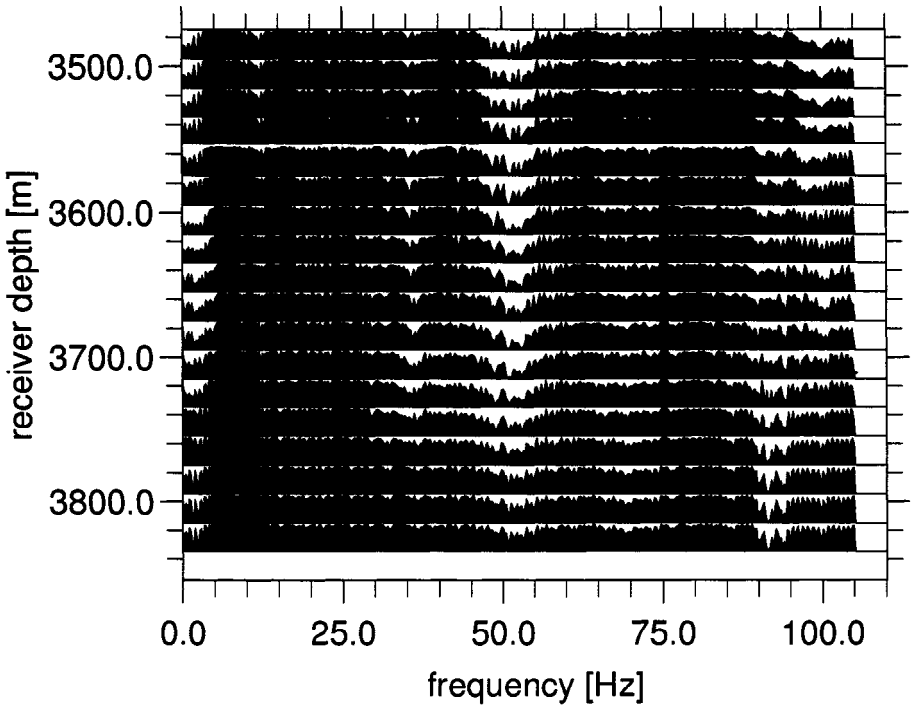

FIG. 5. Frequency-domain semblance for the data from Figure 1.

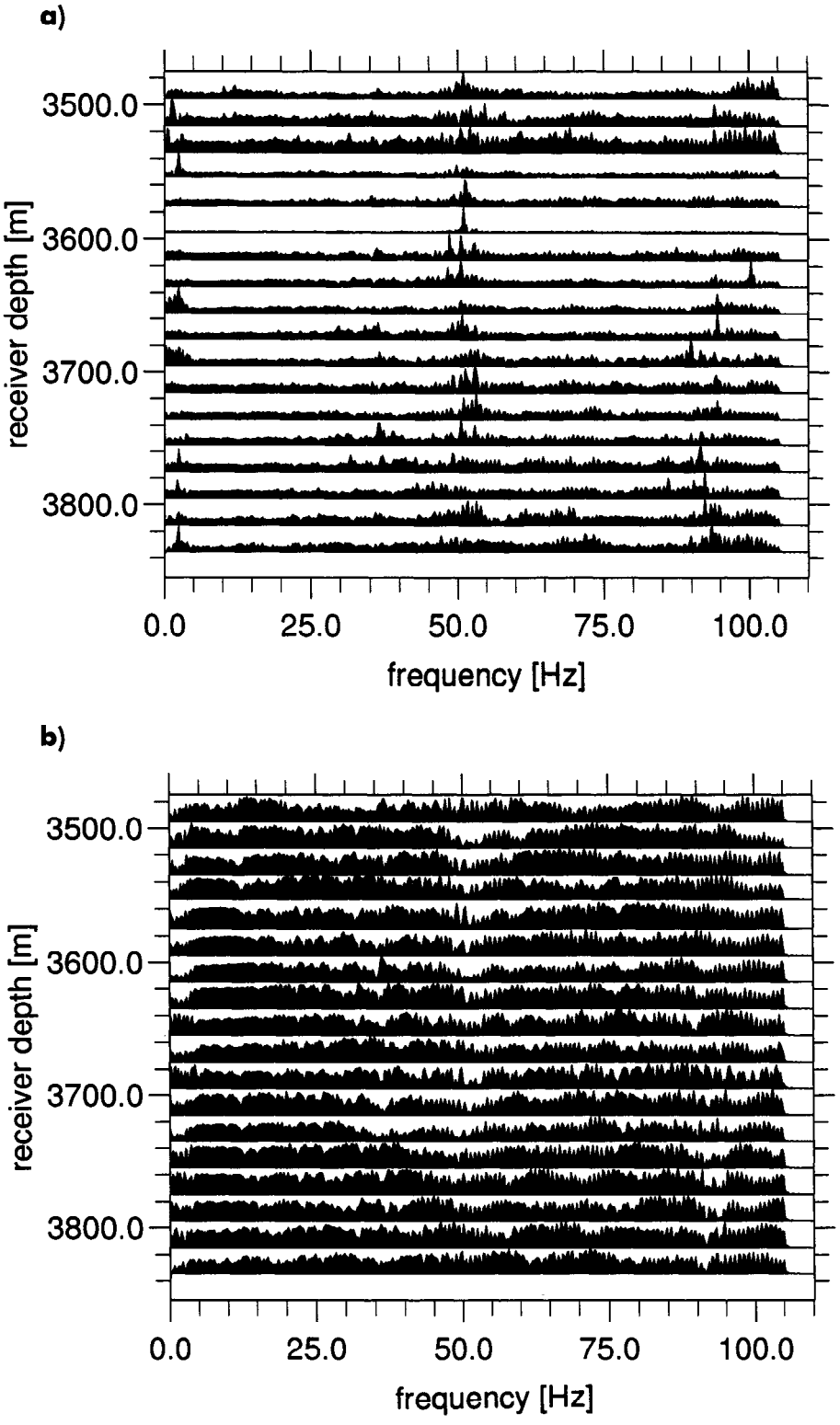

FIG. 6. Amplitude spectra of deconvolved VSP data. (a) Without semblance weighting. (b) With semblance weighting applied. Display is normalized trace by trace.

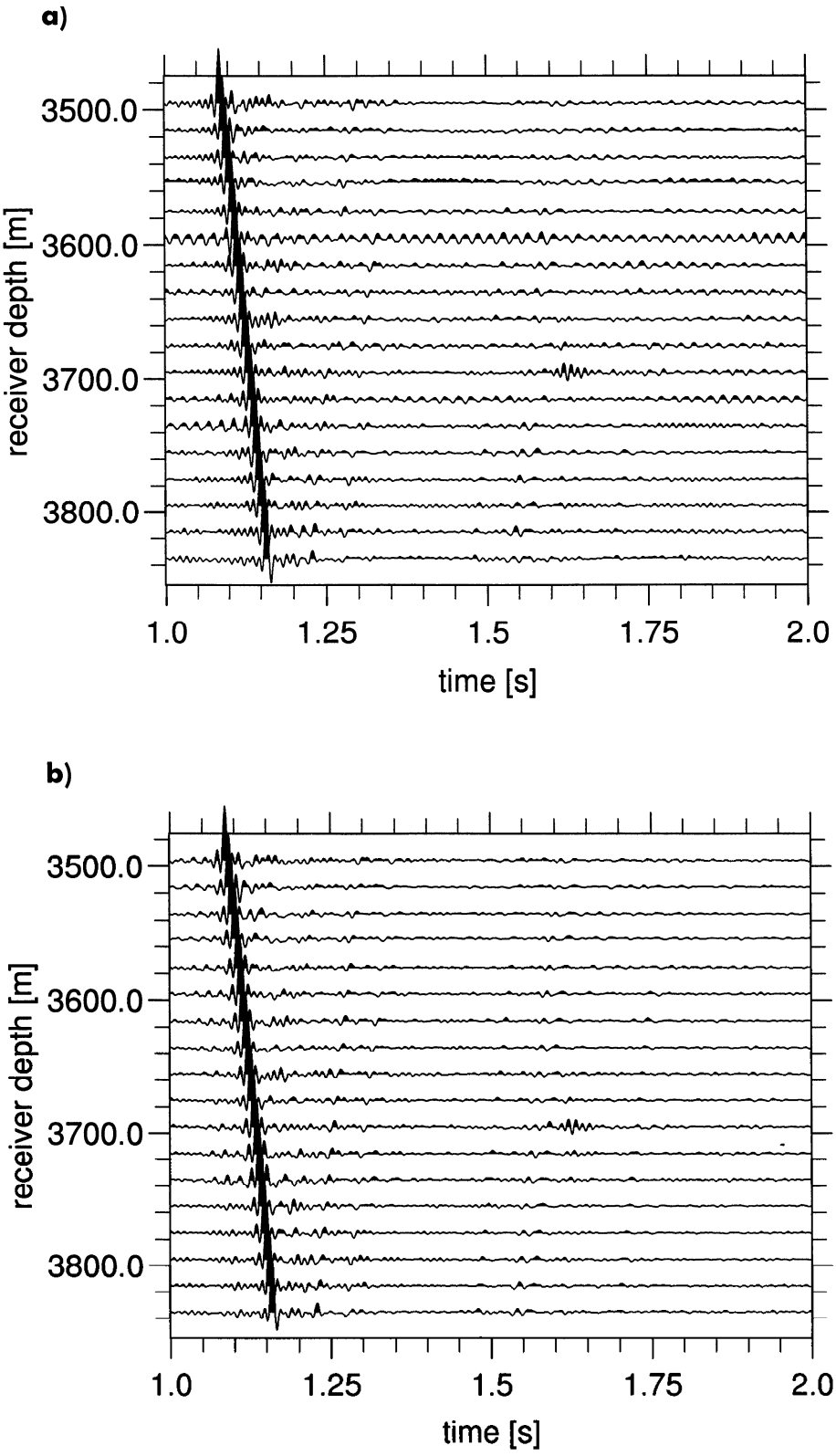

FIG. 7. The total field after the application of the optimum deconvolution operator defined by equation (16): (a) Without semblance weighting. (b) With semblance weighting applied. Display is normalized trace by trace.

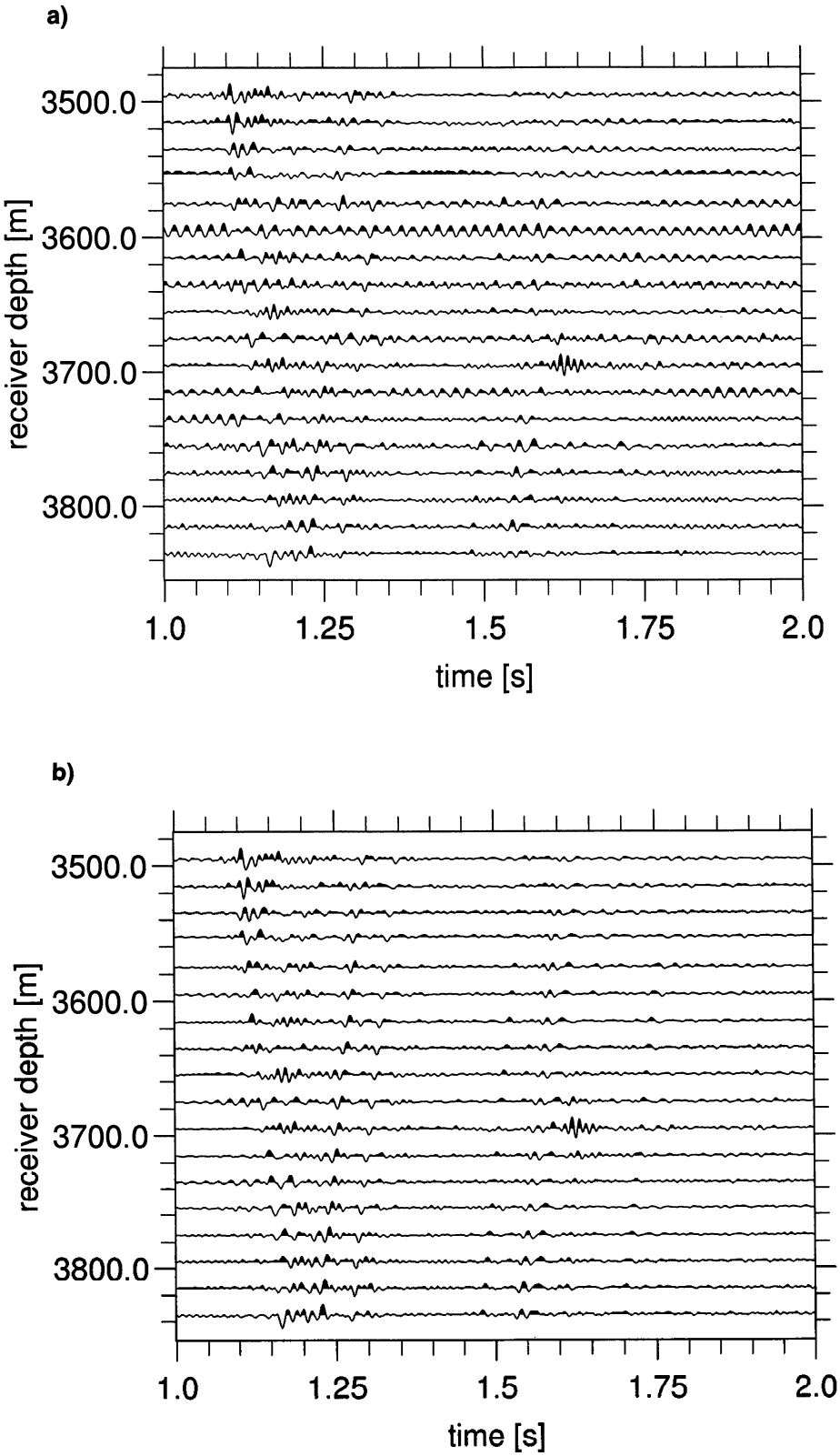

FIG. 8. The residual field obtained by subtracting the deconvolved direct field from the deconvolved total field: (a) Without semblance weighting. (b) With semblance weighting applied.

optimum inverse operator was applied. The frequency averaging is done over the processing band from 0 to 105 Hz. The energies are the average over the total array.

We see that about 95 percent of the total energy is contained in the direct arrivals. We achieved a reduction of about 20 percent in the noise energy. A visual inspection of Figure 6 confirms that the energy removed represents a substantial portion of the total, incoherent energy, and that the residual "noise" is, in fact, reflected energy.

The average semblance is 0.90, meaning that the effective bandwidth of the signal after deconvolution is 95 Hz, or 90 percent of the 105Hz band used in the processing.

DISCUSSION

In the example, when omitting the semblance term from the deconvolution filter, we added just enough white noise to the denominator to stabilize the filter. By choosing the noise and band-limiting parameters for a conventional deconvolution filter [e.g., Berkhout (1977), equation (27)] it can be made to perform much better and may, with appropriate parameters, approach the optimum inverse filter (14) as a limit. However the filter (14) attains the "best possible" result (in a least squares sense) automatically and without the subjective and labor intensive step of selecting filter parameters. Applied in a spatially sliding time window, the optimum inverse filter will allow each single trace its maximum coherent bandwidth.

CONCLUSIONS

The application demonstrates that optimal, focused array deconvolution is an effective technique for processing VSPs

Table 2. Relative signal energy for the frequency interval fron 0-105 Hz from the processing of the zero-offset VSP using th expressions listed in Table 1.

	Before deconvolution	After deconvolutiol
Average semblance	0.90	0.90
Signal-to-total energy	0.94	0.95
Signal-to-noise energy	15.3	20.2

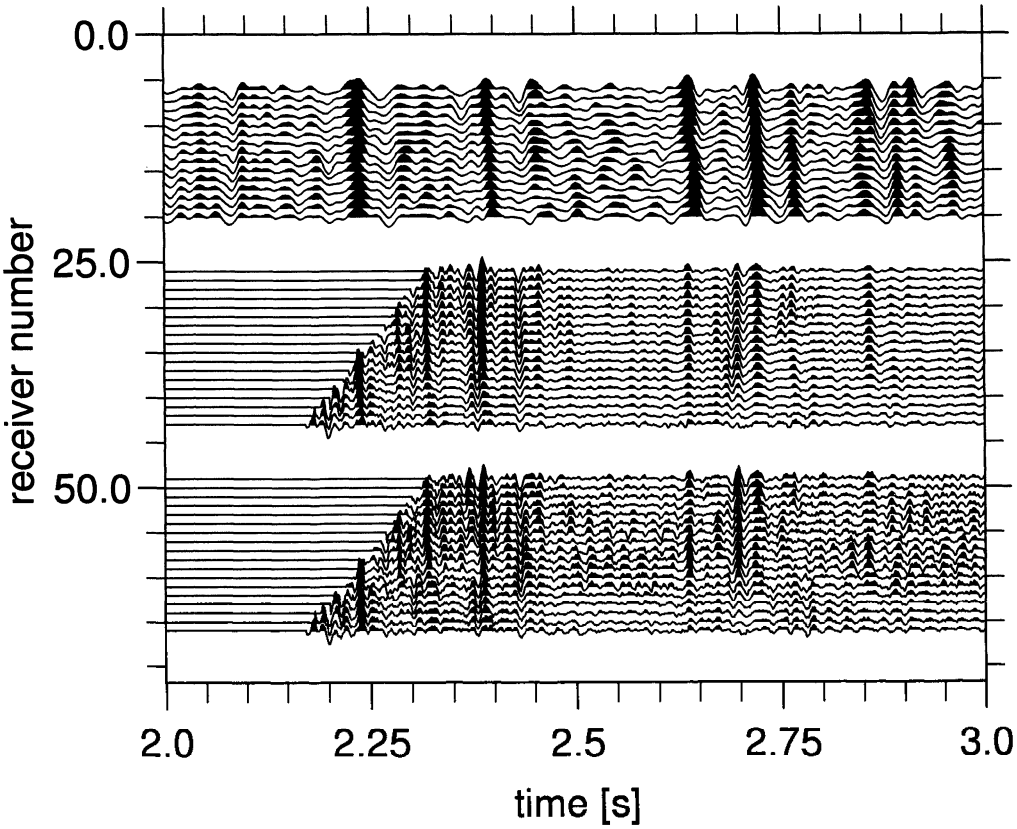

FIG. 9. Deconvolved VSP data in two-way time, processed (left) without semblance weighting, and (center) with semblance weighting applied. To the right: nearby traces from the migrated surface seismic section. The well is close to the leftmost of the surface-seismic traces. Display is normalized trace by trace.

In conventional deconvolution processing, the filter is stabilized by additive white noise, and the noise in the deconvolved data is reduced by subsequent band limiting and notch filters. For the optimum deconvolution filter described in this paper, the filter stabilization is not needed and the postdeconvolution noise is automatically, data-adaptively and optimally attenuated, thus eliminating an often subjective and labor-intensive step from the processing of VSP data. The resulting deconvolved data will be limited to the bands of frequencies that carry significant signal.

It followed from the general properties of the inverse filter that one needs a seismic source with the same spectrum as the noise to get a deconvolved signature with a flat spectrum.

ACKNOWLEDGMENTS

We are indebted to H.-J. Zoch of RWE-DEA and Prof. Dr. R. Marschall of GECO-PRAKLA for collaboration in planning the experiment during which the data we have presented here were collected, and we would like to thank BEB, RWE-DEA, Mobil, Preussag, and WIAG for releasing the data for publication.

REFERENCES

Andrews, A. C., and Hunt, B. R., 1977, Digital image restoration: Prentice-Hall, Inc.

Berkhout, A. J., 1977, Least-squares inverse filtering and wavelet deconvolution: Geophysics, 42, 1369-1383.

DiSiena, J. P., Byun, B. S., and Fix, J. E., 1980, Vertical seismic profiling, a processing analysis case study: Presented at the 50th Ann. Internat. Mtg., Soc. Expl. Geophys.

Haldorsen, J., Miller, D., Walsh, J., and Zoch, H.-J., 1992, A multichannel approach to signature estimation and deconvolution for drill bit imaging: 62nd Ann. Intemat. Mtg., Soc. Expl. Geophys., 181-184.

Hardage, B . A., 1985, Vertical seismic profiling, in Helbig , K., and Treitel, S., Eds., Handbook of geophysical exploration, Section I. Seismic exploration, vol. 14A, Chapt. 5: Geophys. Press.

Kennet, P., Ireson, R. L., and Conn, P. J., 1980, Vertical seismic profiles: Their applications in exploration geophysics: Geophys. Prosp., 28, 676-699.

Miller, D., Haldorsen, J., and Kostov, C., 1990, Methods for deconvolution of unknown source signatures from unknown waveform data: U.S. Patent 4 922 362.

Miller, D., Oristaglio, M., and Beylkin, G., 1987, A new slant on seismic imaging: migration and integral geometry: Geophysics, 52, 943-964.

Seeman, B., and Horowitz, L., 1983, Vertical seismic profiling: Separation of upgoing and downgoing acoustic waves in a stratified medium: Geophysics, 48, 555-568.